GEOPHYSICS, VOL. 65, NO. 5 (SEPTEMBER-OCTOBER 2000); P. 1514–1526, 10 FIGS., 2 TABLES.

Application of gravity and magnetic methods to assess geological hazards and natural resource potential in the Mosida Hills, Utah County, Utah

Alvin K. Benson* and Andrew R. Floyd‡

ABSTRACT

Gravity and magnetic data were collected in the Mosida Hills, Utah County, Utah, at over 1100 stations covering an area of approximately 58 km^2 (150 mi^2) in order to help define the subsurface geology and assess potential geological hazards for urban planning in an area where the population is rapidly increasing. In addition, potential hydrocarbon traps and mineral ore bodies may be associated with some of the interpreted subsurface structures. Standard processing techniques were applied to the data to remove known variations unrelated to the geology of the area. The residual data were used to generate gravity and magnetic contour maps, isometric projections, profiles, and subsurface models. Ambiguities in the geological models were reduced by (1) incorporating data from previous geophysical surveys, surface mapping, and aeromagnetic data, (2) integrating the gravity and magnetic data from our survey, and (3) correlating the modeled cross sections. Gravity highs and coincident magnetic highs delineate mafic lava flows, gravity lows and magnetic highs reflect tuffs, and gravity highs and magnetic lows spatially correlate with carbonates. These correlations help identify the subsurface geology and lead to new insights about the formation of the associated valleys. At least eight new faults (or fault segments) were identified from the gravity data, whereas the magnetic data indicate the existence of at least three concealed and/or poorly exposed igneous bodies, as well as a large ash-flow tuff. The presence of low-angle faults suggests that folding or downwarping, in addition to faulting, played a role in the formation of the valleys in the Mosida Hills area. The interpreted location and nature of concealed faults and volcanic flows in the Mosida Hills area are being used by policy makers to help develop mitigation procedures to protect life and property.

INTRODUCTION

The Mosida Hills, Utah County, Utah, is a low range of hills to the west of Utah Lake that connect the southern end of the Lake Mountains with the northern end of the East Tintic Mountains (Figures 1, 2). With the rapid growth in population in Utah County, future housing development in the Mosida Hills area is inevitable. Associated with this development is the probability of zoning requests for higher density housing. The potential risk of this development necessitates accurate mapping of the subsurface geology to locate potential hazards, particularly faulting. Based on the surface geology, assessments by Gori (1993) and Robison (1993a, b) indicate significant potential for surface rupture, deformation, and slope movement west of the Mosida Hills. Clearly, there is a threat to lives and property in the Mosida Hills area due to potential large earthquakes that might occur along preexisting zonest of weakness or faults. Buildings straddling faults could be ripped apart during an earthquake. In order to mitigate damage to property and loss of lives, the locations of individual faults within the Mosida Hills fault zone should be determined as accurately as possible (Gori, 1993).

In the past, detection of faults in the Mosida Hills has been limited primarily to observations of surface features, but many fault traces have been obliterated by geological and cultural events. Consequently, this study focuses on hazard detection using geophysical methods. The resulting interpretations will be used in future master planning and subdivision approvals (J. Grover, personal communication, 1999). By knowing where faults exist in the subsurface, buildings can be set back so that they do not straddle a fault line. Given an adequate setback distance, modern construction methods can protect against shaking damage.

Manuscript received by the Editor March 5, 1999; revised manuscript received January 10, 2000.
*Brigham Young University, Dept. of Geology and Geophysics, S-321 ESC, Provo, Utah 84602-4606. E-mail: alvin_benson@byu.edu.
‡University of Nevada, Reno, Dept. of Geological Sciences, Reno, Nevada 89557. E-mail: arf@seismo.unv.edu.

Although the risk is low, volcanic threats also exist in the Mosida Hills area. Hazards expected to accompany possible future volcanic activity include loss or reduction of agricultural and recreation lands; obstruction of transportation, communication, and power facilities; and damage or destruction to proximate buildings. Life-threatening hazards are not expected, but daily routines could be disrupted by lava flows where communities are near active vents. Understanding volcanic processes, locations of lava flows, and identification of potentially active eruptive centers are necessary to help formulate mitigation procedures.

Gravity and magnetic data were collected at more than 1100 stations (Figure 2) to help map the subsurface geology. The primary objectives of this study are to integrate the gravity and magnetic data from the Mosida Hills area in order to (1) delineate and map concealed faults, (2) determine the horizontal extent and possible source of the volcanic rocks, (3) better understand Basin and Range faulting, (4) provide the interpreted data to policy makers and engineers to help with planning and development of land, and (5) provide interpreted geophysical data to help assess potential hydrocarbon traps and mineral ore bodies. The integration of gravity and magnetic data reduces ambiguity by providing more rock characteristics to help map structure and distinguish general lithologies.

Previous work in the study area has primarily involved surface geologic mapping by Rigby (1949, 1952), Bullock (1951), Hoffman (1951), Williams (1951), Morris and Lovering (1961), F. D. Davis (unpublished data, 1981), Hintze (1988), and P. D. Proctor (unpublished data, 1985 and 1990). Their work shows that the Mosida Hills consist primarily of folded Paleozoic carbonate rocks, while volcanic rocks consist of Tertiary tuffs and lava flows.

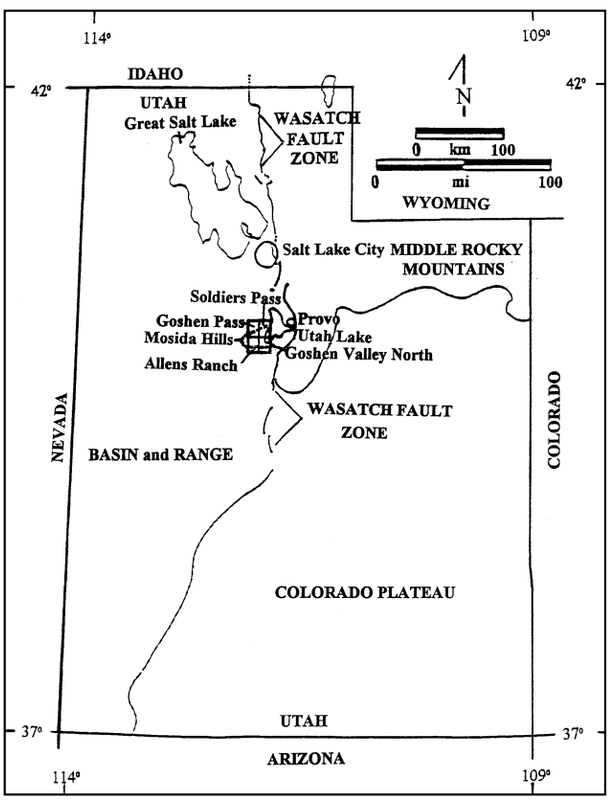

FIG. 1. Index map showing the location the four quadrangles which contain the Mosida Hills, west of Utah Lake and Provo, Utah.

A regional gravity survey conducted by Cook and Berg (1961) over the central part of Utah included about 50 widespread stations within the Mosida Hills area. Based upon the presence of a probable bounding fault along the western margin of Goshen Valley, they postulated that Goshen Valley may be a graben separating West Mountain and the Mosida Hills. They agreed with Bullock (1951) that Cedar Valley is a "structural valley," or large downwarp, that is locally accentuated by faulting. However, their interpretations were qualitative, and they suggested that future geophysical work would better establish a representation of the subsurface geology.

Other geophysical work done in this part of the Basin and Range province include regional gravity surveys by Davis (1983), Zoback (1983), and Cook et al. (1997). Davis (1983) constructed two gravity models across the south-central portion of Goshen Valley to the east of the East Tintic Mountains, and she agrees with the conclusions of Cook and Berg (1961). Zoback (1983) was primarily concerned with the structure and tectonism of the Wasatch fault zone in the Salt Lake City area. However, she interprets bounding faults along the east and west margins of Cedar and Goshen Valleys. The gravity data were modeled along selected profiles, but Zoback pointed out that data throughout much of the area were too sparse; as a consequence, detailed subsurface structure could not be determined. She suggested that more detailed geophysical surveys be conducted in this area in the future.

GEOLOGIC SETTING—STRATIGRAPHY AND STRUCTURE

Although the Mosida Hills are composed primarily of Paleozoic carbonate rocks (286–525 Ma), two major noncarbonate units are the Manning Canyon Shale (325 Ma) and the Butterfield Peaks Formation (a large sandstone component; 305 Ma). Both of these units are found exposed to the north in the Lake Mountains. The Paleozoic rocks range in age from the Cambrian Cole Canyon Dolomite (520 Ma), exposed along the northern end of the East Tintic Mountains in the southern end of the Mosida Hills, to the Pennsylvanian Butterfield Peaks Formation (305 Ma) of the Oquirrh Group, exposed in the Lake Mountains at the northern end of the Mosida Hills area (Figure 2).

The Tertiary rocks (12.1–44.3 Ma) are mostly volcanic in origin, but include some gravels and nonmarine, or lacustrine, limestone deposits. The Quaternary deposits are composed of Lake Bonneville sediments and recent alluvial fan deposits. These deposits cover much of the relevant geology in the area.

There are several mafic lava flows (17.3–32.6 Ma) in the Mosida Hills area, but none have been named or included in a formal stratigraphic unit. These flows are located at the northern end of the Mosida Hills just south of Soldiers Pass (Figure 2), where they lie directly on one another and are interbedded with lacustrine limestone.

The structural elements of the Mosida Hills area, as described by Rigby (1949, 1952), Hoffman (1951), and Williams (1951), consist of asymmetrical anticlines and synclines along

with normal, reverse, and thrust faults located within the Paleozoic section. The folds are fairly tight, with the axial planes dipping to the west and striking roughly to the north. Rigby (1949, 1952), Hoffman (1951), and Williams (1951) all interpret the folding to be associated with thrust faulting, and it appears that both the folding and the faulting probably occurred during the Sevier Orogeny.

The upthrown blocks of the north-striking faults in Cedar Valley and in Goshen Valley are most likely composed of Paleozoic carbonate rocks, whereas the downthrown block (which is also carbonate rock) is probably covered by a sequence of low-density, valley-filling sediments. The depth of the valley fill would therefore provide a minimum value for the amount of vertical offset. Due to the large density contrasts (>0.5 g/cm^3) and possible magnetic susceptibility contrasts between the valley fill, the carbonate rocks, and the tuffs, this type of faulting should be detectable from gravity and magnetic data.

GEOPHYSICAL ANALYSIS

Data collection and processing

Gravity and magnetic data were collected at 1117 stations during the early to mid-1990s (Figure 2). Locations were determined from available maps, along with recorded vehicle mileage from known reference points. Latitudes, longitudes, and elevations were read at every station with a Trimble GPS receiver capable of real time corrections. These readings were corroborated with those taken from available blue line maps with a scale of approximately 1:6000 and a contour interval of 1.5 m (5 ft). Stations located on bedrock were not only collected within the Mosida Hills area, but also along the ranges west and east of the Mosida Hills area, including mountains east of Utah Lake, in order to facilitate regional corrections to the data. Due to the access difficulties, minimal data were collected at Utah Lake and the higher elevations of the East Tintic and Lake Mountains.

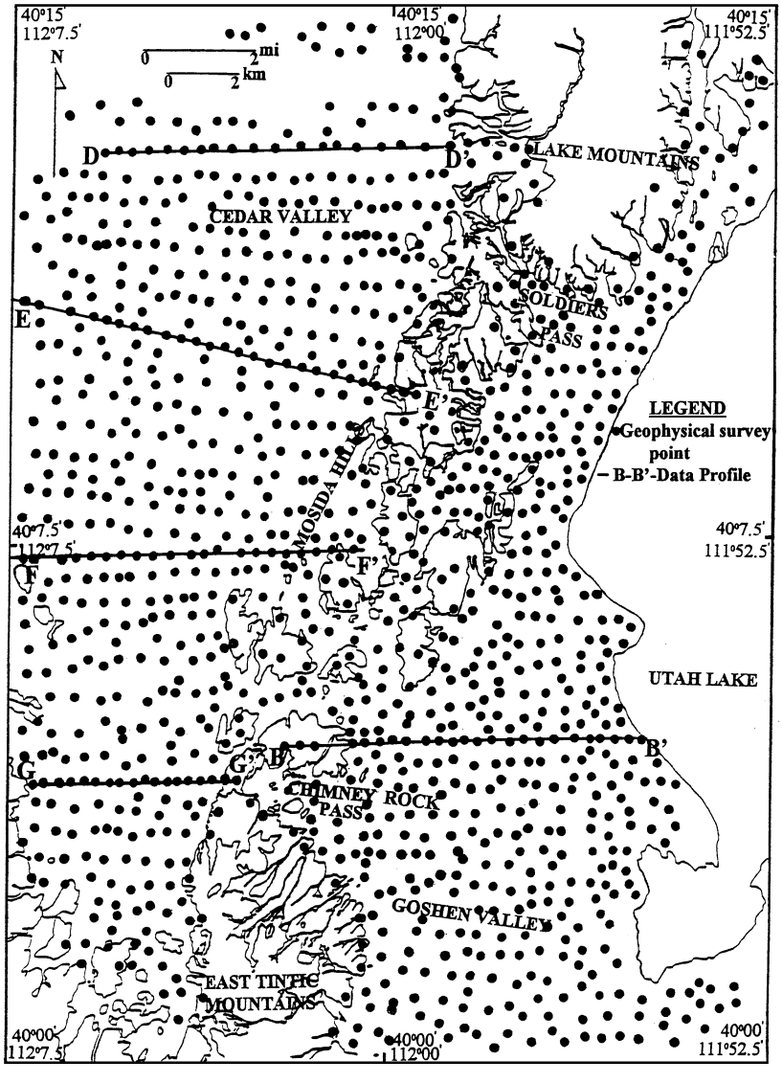

FIG. 2. Index map showing the location of the Mosida Hills, the location of 1117 stations where gravity and magnetic data were acquired, and some selected profiles. Gravity and magnetic data obtained along profiles DD', EE', FF', GG', and BB' are modeled and interpreted in this paper.

A Worden gravimeter was used for the gravity measurements; a Geometrics proton-precession magnetometer was used for the magnetic field measurements. Care was taken to minimize measurement errors, and any dubious measurements were double checked. Repeated gravity measurements, using the looping technique, showed a maximum error of 0.25 mGal due to drift. The maximum error associated with elevation determination was 0.9 m (3 ft), resulting in a possible error of 0.27 mGal. Latitudes were determined within 9 m (30 ft), leading to a maximum error of 0.008 mGal, while the accuracy of terrain corrections was 1 m (3.3 ft), or 0.30 mGal. Thus, the estimated maximum error in residual gravity values would be approximately 0.83 mGal, but it is unlikely that these maximum errors would occur at any one station. At least five magnetic readings were taken at each station and averaged. Typically, the largest variation in the readings at any station was only 8–10 nT (gammas). Thus, cultural or other types of magnetic "noise" were minimal in this study.

The data were processed using standard techniques, with some modifications made to the Bouguer and terrain corrections. The gravity data were processed to remove meter drift and variations due to differences in latitude, elevation, and topography. When making the Bouguer correction, two assumptions are typically applied: (1) the density of the intervening slab of rock between the station being corrected and the reference datum is assumed to be of uniform density, and (2) the slab is of infinite horizontal extent. Neither assumption is really valid. In the first assumption, the density is usually taken as the average density of the terrain surrounding the station. If there are significant local variations in the lithology, using an average density can introduce considerable error (Dobrin and Savit, 1988). The best reduction values are determined by sampling rocks and sediments from the survey area and determining the densities in the laboratory (Telford et al., 1990). For example, White (1949) used three different densities within a small area for Bouguer and terrain corrections for gravity data collected in southern England. Based on rock samples taken from the Mosida Hills site (83 representative samples over the site) (Table 1) and the Parasnis (1962) method, near-surface densities were determined to be 1.8–1.95 g/cm^3 near the centers of Cedar Valley and Goshen Valley. Approximately 1.6–2.4 km either west or east from the center of these valleys, near-surface densities range from 2.31 to 2.42 g/cm^3. In the Boulter Mountains to the west, the Lake Mountains to the north, the East Tintic Mountains to the south, West Mountain to the east of Utah Lake, and in the Mosida Hills, near-surface densities densities range between 2.63 and 2.71 g/cm^3. Wherever available, densities determined in the lab were used for the Bouguer correction. Otherwise, near-surface densities were linearly graded from the valley centers to the mountain ranges and used for making the Bouguer correction. Smooth gradation was used to eliminate any anomalies that might be generated by introducing abrupt changes in near-surface densities. Since finite slabs of varying density were used for the Bouguer correction, the mathematical expression for a truncated slab was used instead of that for an infinite slab (Telford et al., 1990; Burger, 1992). For terrain corrections, the density used for each compartment in the Hammer template was determined from rock samples or from the Parasnis (1962) method applied to a group of sectors. The correction factor was multiplied by the angle associated with the compartment or group of sectors versus 2π (Telford et al., 1990). This approach produced good results for gravity and magnetic data studies 4–8 km east of Utah Lake, yielding the best correlation between final subsurface models and ground truth based on trench studies (Benson and Mustoe, 1991, 1995; Benson and Hash, 1998).

Table 1. Densities of rock samples from the Mosida Hills area.

Rock Type	Number of Samples	Density (g/cm^3)	Standard deviation (g/cm^3)
Rhyolitic tuff	15	1.76–2.28	0.19
Nonmarine limestone	17	2.44–2.55	0.21
Mafic lava flows	21	2.74–2.86	0.23
Quartzite	10	2.69–2.70	0.25
Limestone	20	2.64–2.67	0.22

The magnetic data were corrected for diurnal variations in the earth's magnetic field and for latitude variations using International Geomagnetic Reference Field (IGRF) data. Because the Zeng (1989) method provides a quantitative estimate for choosing the optimal polynomial order for the regional correction, it was used to separate reduced anomaly values into regional and residual components. For our gravity and magnetic data, the highest order polynomials determined from the Zeng approach were second order. The polynomial functions were determined using surface trend analysis (Burger, 1992). Subtraction of the regional polynomial from the reduced anomaly values produced the residual values. The residual gravity and magnetic values were contoured and used to help model and interpret the subsurface geology.

CONTOUR MAPS

Contour maps (Figures 3, 4) were constructed from the residual gravity and magnetic data. The characteristic gravity profile signature for a fault is a steep gradient flanked by shallower gradients. Steep gravity gradients along the margins of the ranges most likely represent normal faults, and several negative gravity anomalies occur in the valleys (Figure 3). Two small valleys, one just south of Soldiers Pass and the other in Chimney Rock Pass, extend across the Mosida Hills. These probably represent east-west valleys or depressions filled with lower density material that existed prior to Basin and Range faulting. These depressions were probably cut by north-south Basin and Range faults, with some portions of these valleys being downdropped and buried, and other portions being uplifted to form part of the range. It also appears that there is a continuous range connecting the East Tintic Mountains with the Lake Mountains (Figures 2, 3). Based upon hydrocarbon shows in a well east of the Mosida Hills area (Benson and Hash, 1998), some of the faulted bedrock highs along eastern and western portions of Cedar Valley may represent potential hydrocarbon traps (Figures 3, 5–8).

Two positive residual gravity anomalies in the Mosida Hills near Chimney Rock Pass have about the same magnitude (+10 and +8 mGal) and are offset. They may have been one anomaly at some previous time. This could be evidence for strike-slip faulting, as suggested by P. D. Proctor (unpublished data, 1985, 1990). Although the offset appears to be in the northeast-southwest direction, the direction cannot be precisely determined from the contoured gravity data.

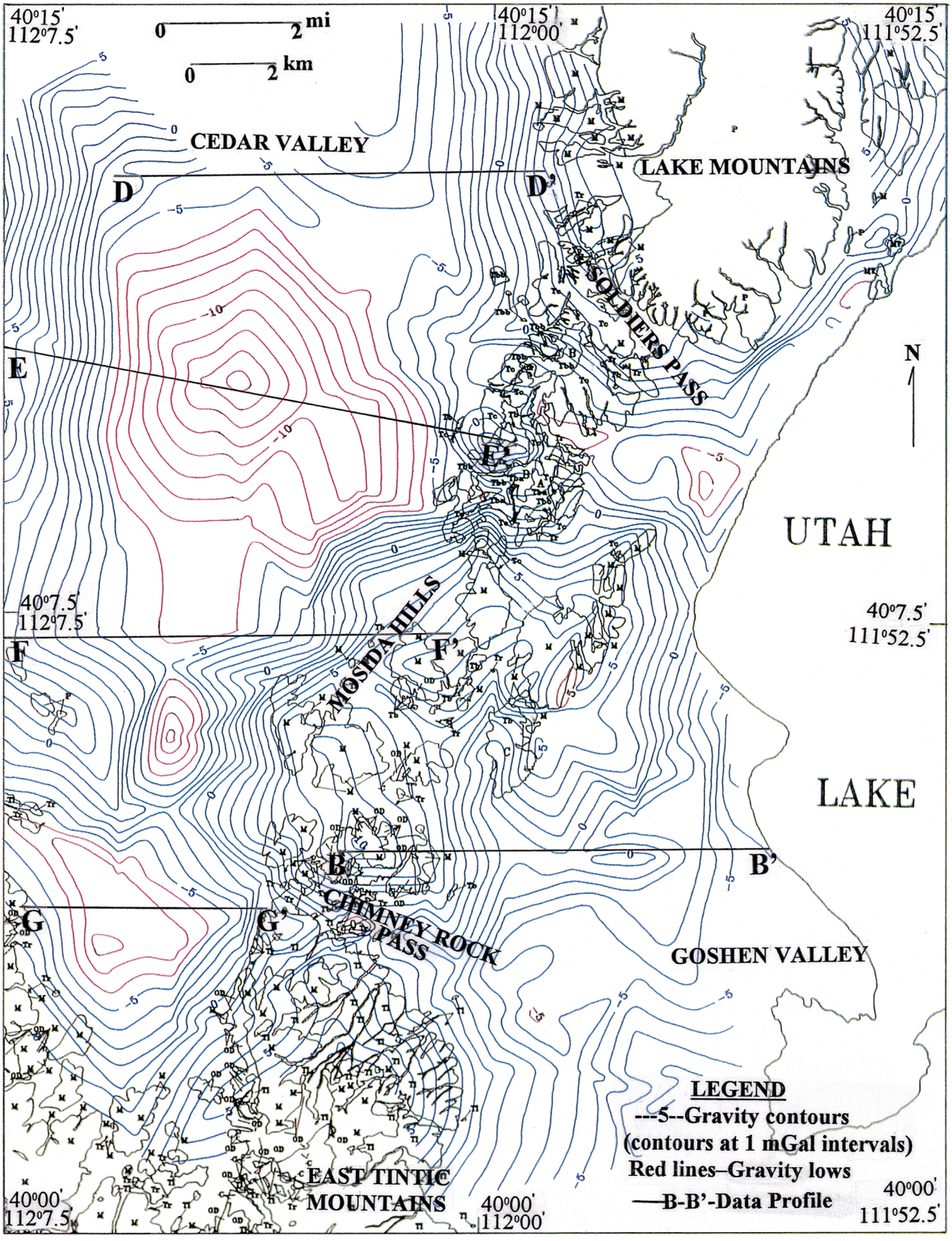

FIG. 3. Residual gravity contour map in the Mosida Hills study area. Contour interval = 1 mGal. Steep gravity gradients indicate the presence of faulting. Blue lines correspond to gravity highs, red lines to gravity lows. Tc = Tertiary carbonate rock; Tb = Tertiary mafic flows; Tba = basaltic trachyandesite; Tbb = Trachybasalt; Tl = Tertiary Laguna Springs Formation; Tr = Tertiary rhyolitic ash-flow tuffs; P = Pennsylvanian sedimentary rocks, mostly carbonates; M = Mississippian sedimentary rocks, mostly carbonates; OD = Ordovician through Devonian sedimentary rocks, mostly carbonates; C = Cambrian sedimentary rocks, mostly carbonates.

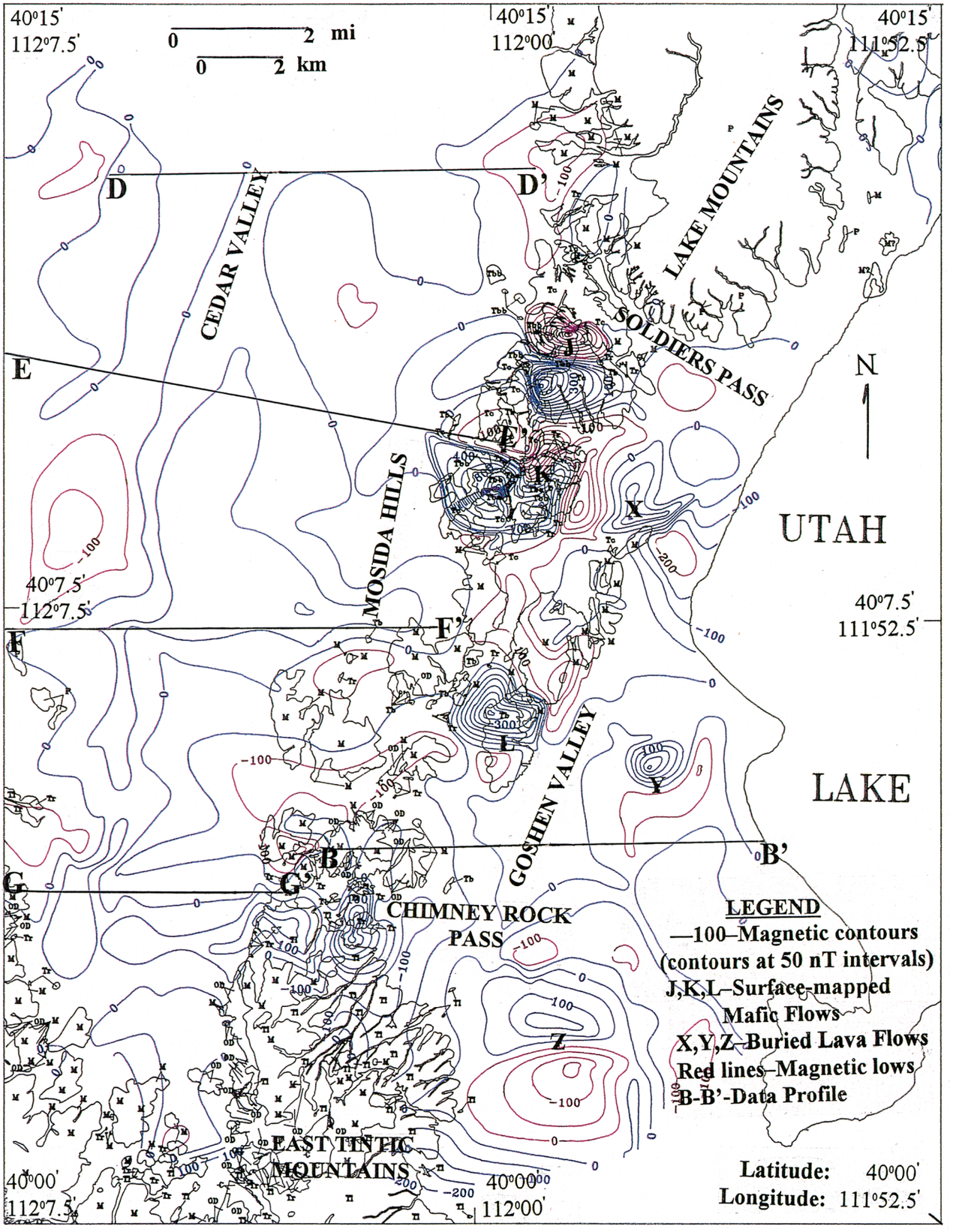

FIG. 4. Residual magnetic contour map in the Mosida Hills study area. Contour interval = 50 nT. J, K, and L are surface-mapped mafic lava flows; X, Y, and Z appear to represent buried lava flows. Blue lines correspond to magnetic highs, red lines to magnetic lows. Lithology abbreviations are as in Figure 3.

Analysis of the magnetic contour map shows that the surface-mapped mafic lava flows (J, K, and L; Figure 4) are each represented by a large localized magnetic anomaly. These flows appear to be associated with previous volcanic activity in the Mosida Hills, and some potential active vents may still be present (P. D. Proctor, unpublished data and personal communication, 1998). Similarly, the three magnetic anomalies (X, Y, and Z; Figure 4) in Goshen Valley most likely represent buried lava flows that originated within the Mosida Hills. Anomaly Y, with an upper surface area of approximately 0.5 km^2, may be a downfaulted portion of lava flow L. The separation is possibly caused by erosion prior to faulting, but since a gravity high separates them, it is more likely a structural ridge acting as a barrier to lava flow. Aomaly X, with an upper surface area

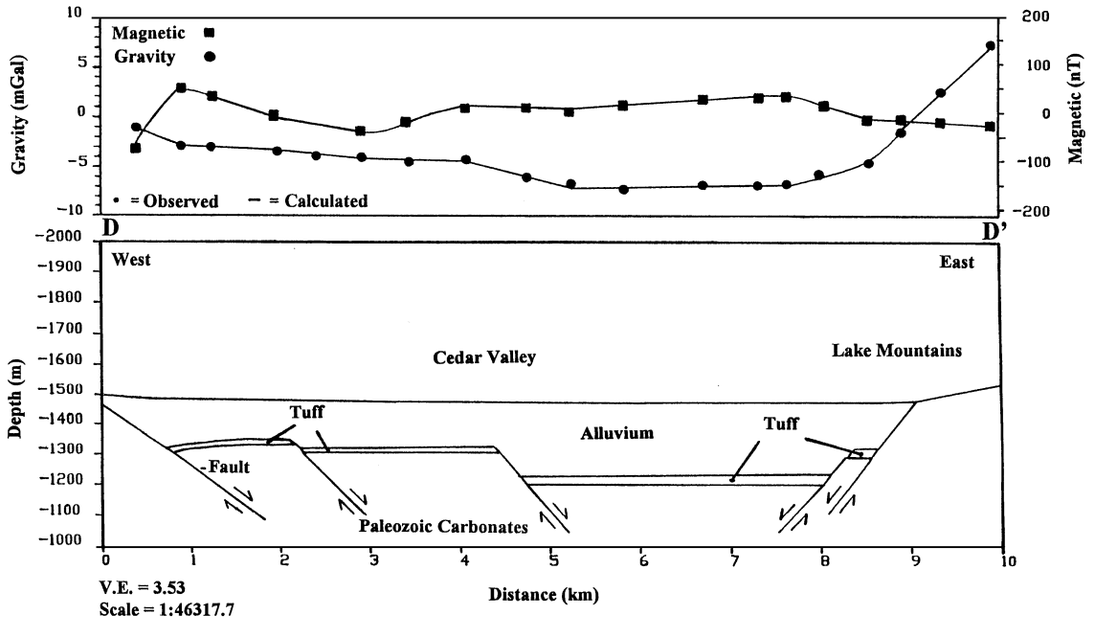

FIG. 5. Residual gravity and reduced magnetic data along profile DD' (for location, see Figure 2). The modeled gravity and magnetic data are generated from a geological model with an antithetic fault on the western side. Since the vertical exaggeration is 3.53, two of the five interpreted faults have real dips less than 20°. Real dips range between 12° and 22°.

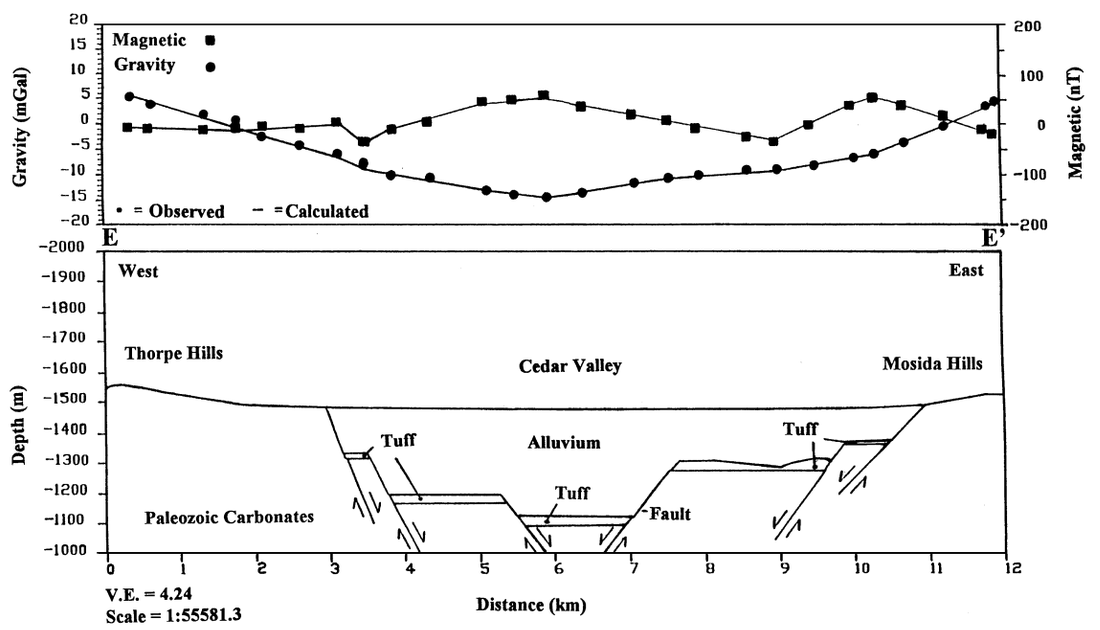

FIG. 6. Residual gravity and reduced magnetic data along profile EE' (for location, see Figure 2). The modeled gravity and magnetic data are generated from a geological model showing faulting along the western and eastern margins of Cedar Valley. Since the vertical exaggeration is 4.24, four of the six interpreted faults have real dips less than 20°. Real dips range between 14° and 33°.

of approximately 0.35 km^2, possibly represents a dipolar body containing some remanent magnetization, but it is more likely associated with a reversed polarity flow. The southern anomaly (Z), with an upper surface area of approximately 1.3 km^2, is not as localized as the others, and its dipolar nature suggests that it may also contain some remanent magnetization, as well as being rotated from its original attitude. This type of anomaly may be a result of deeper burial beneath the valley fill. Initial assessments indicate that mineral deposits, which include silver, zinc, and lead, may be associated with the interpreted igneous bodies (J, K, L, X, Y, Z; Figure 4), as well as with some of the interpreted faults near the East Tintic Mountains and West of the Lake Mountains (P. D. Proctor, unpublished data, 1998).

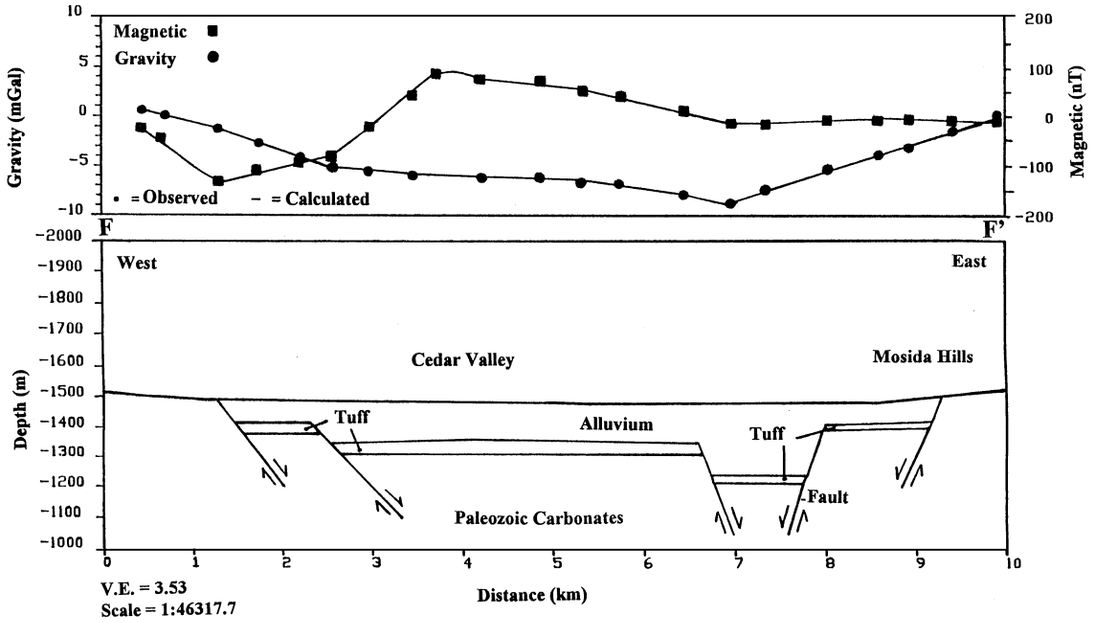

FIG. 7. Residual gravity and reduced magnetic data along profile FF' (for location, see Figure 2). The modeled gravity and magnetic data are generated from a geological model containing a tuff with nonuniform thickness. Since the vertical exaggeration is 3.53, one of the five interpreted faults has a real dip less than 20°. Real dips range between 18° and 36°.

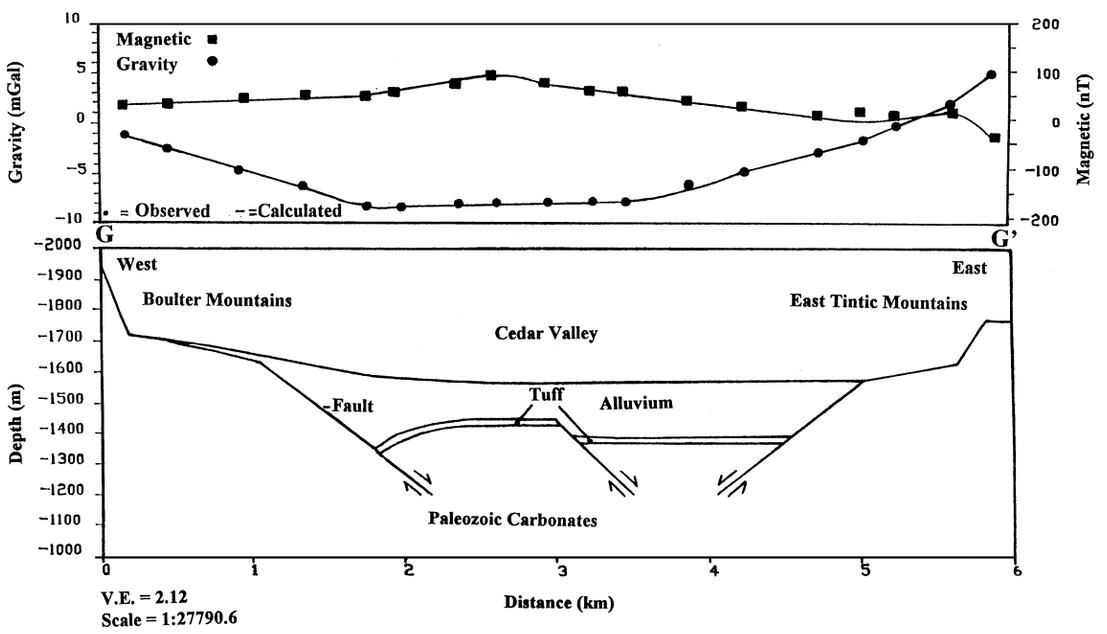

FIG. 8. Residual gravity and reduced magnetic data along profile GG' (for location, see Figure 2). The modeled gravity and magnetic data are generated from a geological model showing similar reverse drag faulting as in profile DD' (Figure 8). The vertical exaggeration is 2.12, and none of the three interpreted faults have real dips less than 20°. Real dips range between 20° and 26°.

Where the ash-flow tuffs are exposed in Chimney Rock Pass, the magnetic signature is generally lower in amplitude and longer in wavelength than the lava-flow anomalies. This is probably due to the tuffs having a lower magnetic susceptibility or some remanent magnetization and a more extensive lateral distribution. The small magnetic high that extends along the length of Cedar Valley is indicative of this type of anomaly and may represent a tuff deposit buried in Cedar Valley, with an approximate upper surface area of 20 km^2. Although the magnetic-anomaly patterns are not as helpful in identifying specific structures as are the gravity data, they do indicate where igneous bodies are located. In addition, it is apparent that many of the magnetic lows correspond to outcrops of Paleozoic carbonate rocks.

STRUCTURAL MODELS OF THE MOSIDA HILLS AREA

Modeling parameters

Before quantitative modeling could be done, representative values of density and magnetic susceptibility for the different rock types in the Mosida Hills area were determined. Over eighty rock samples (Tables 1, 2) were collected representing each of the different rock types at various locations throughout the Mosida Hills area.

The dry bulk densities of the rock samples were measured in the laboratory using Archimedes' method [dry sample weight/(dry sample weight − submerged sample weight)], and values are summarized in Table 1. The large variations in tuff densities are due to changes in pumice content and to some extent to the degree of welding. Tuff samples with larger and more abundant pumice had lower densities, whereas the opposite was true of tuff samples with smaller and less abundant pumice.

The magnetic susceptibility of the rocks was measured in the field using a Kappameter model KT-5 by Geofyzika Brno, Czechoslovakia. As expected, the susceptibilities are highly variable, especially in the mafic lava flows (Table 2). The variability in magnetic susceptibilities is dependent on several factors. In the case of the rhyolitic tuffs, the tuffs with the larger bulk percentage of pumice and larger pumice clasts have lower susceptibilities. The amount of weathering or alteration also seems to be a factor, especially for the mafic lava flows. The most altered rocks have the lowest susceptibilities, whereas those rocks that were above the highest level of Lake Bonneville looked the least weathered and have the highest susceptibilities. Magnetic susceptibility is highly dependent upon magnetite content. Therefore, compositional variations of magnetic composition within a lava flow or tuff can also be responsible for magnetic susceptibility variations, as can remanent magnetization.

Table 2. Magnetic susceptibilities for rock samples in the Mosida Hills area.

Rock Type	Number of Samples	Susceptibility $\times 10^3$ (SI)	Standard deviation
Limestone and quartzite	30	0.03–0.06	0.004
Nonmarine limestone	17	0.03–0.14	0.01
Mafic lava flows	21	2.30–37.0	1.51
Lava flow at A	6	7.75–14.2	0.91
Lava flow at B	9	2.30–37.0	1.84
Weathered	4	2.30–2.60	0.34
Least weathered	5	21.6–37.0	1.33
Lava flow at C	6	7.32–12.8	1.05
Rhyolitic tuffs	15	0.09–2.64	0.05

Quantitative modeling

In this paper, five representative, strategically located profiles, DD', EE', FF', GG', and BB' (Figures 2, 3), were analyzed using a 2.5 D version of the GM-SYS modeling software. The models are based on three basic lithologies known to be present: Paleozoic carbonates covered by tuff and valley fill. Model fault geometry conformed to the conceptual models discussed by Stewart (1983). Both planar and listric-type faults were considered. By keeping the models simple and using the geological information available for the Mosida Hills area, reasonable models were generated that fit the residual geophysical data. Ambiguities in the geological models were reduced by (1) incorporating data from previous geophysical surveys (Cook and Berg, 1961; Davis, 1983; Cook et al., 1997), surface mapping (Rigby, 1949, 1952; Bullock, 1951; Hoffman, 1951; Williams, 1951; Proctor, unpublished data, 1985, 1990), and aeromagnetic data; (2) integrating the gravity and magnetic data from our survey; and (3) correlating the modeled cross-sections with one another.

Because many of the ranges in the Mosida Hills area are composed of Paleozoic carbonate rocks, the density of the bedrock component ranges between 2.64 and 2.67 g/cm^3, with a magnetic susceptibility of zero SI units (Tables 1, 2). Benson and Mustoe (1991) and Benson and Hash (1998) used the Parasnis (1962) method to determine a density range of 1.8–1.95 g/cm^3 for valley fill in Utah Valley, which is located just to the east of the Mosida Hills area. Hence, this range was also used for valley fill in the Mosida Hills models. Because most of the magnetite, the principal magnetic mineral originally present in the valley fill may have been altered, or maybe was never there, the valley fill has become less susceptible and was assigned a magnetic susceptibility of zero. Because the densities and magnetic susceptibilities are highly variable for the tuffs (Tables 1, 2), average values for both the density and magnetic susceptibility of the tuffs in the vicinity of the chosen profiles were typically used. Average values for density are 2.1 g/cm^3 and for magnetic susceptibility are 2.0×10^{-4} SI units.

Profile DD' (Figure 5), the northernmost profile, is 10 km long, and its west end is at the western edge of Cedar Valley. The model extends eastward to the western edge of the Lake Mountains. The tuff, though faulted, appears to be a uniform sheet that is approximately 30 m thick along the eastern edge and thins to approximately 20 m in the west. This thinning may be a depositional feature, but may also be due to erosion before burial by valley fill. In addition to faulting, other modeling assumptions considered for the tuff included (1) the tuff was eroded into patches prior to basin fill, (2) the tuff varies laterally and vertically in magnetic properties, (3) the tuff and basement surface are warped and folded rather than faulted, and (4) the tuff was faulted in part prior to basin fill. Some of these assumptions proved difficult to test accurately and, in reality, a combination of these assumptions, along with thickness changes and faulting, is most probable.

The Paleozoic carbonate slopes on both the western and eastern edges of Cedar Valley and various locations in between have little or no tuff on them, but the presence of tuff and lacustrine limestone on ridge tops indicate faulting causing a total vertical displacement of at least 250 m (assuming the tuff in the ranges was originally at the same elevation as the tuff buried in the valley). The two closely spaced faults along the eastern edge of the valley could represent a fault zone of many closely spaced faults that are too small to be distinguished. The interpreted reverse drag fault to the west is most likely curved rather than planar (Hamblin, 1965). Other models were also examined, including an antithetic fault on the western side of the valley, but the reverse drag model provided a better fit to the residual data and a more realistic fault geometry.

Although the faults plotted along profile DD' have apparent dips of 45°–70° (Figure 5) due to the vertical exaggeration of 3.53, the real dips of the faults along this profile are between 12° and 22°. This suggests that in addition to faulting, folding or downwarping played a role in the formation of Cedar Valley. It may also suggest the presence of listric faulting.

Profile EE' (Figure 6) is 12 km long and extends from the Thorpe Hills west of Cedar Valley to the outcrops of Paleozoic carbonates on the eastern edge of Cedar Valley. Faulting is again indicated along the margins of the valley, but the fault pattern is more complex than the previous profile. The tuff has a uniform thickness of approximately 30 m with variations most likely due to erosion. Using the tuff as a reference, the amount of offset associated with faulting reaches a maximum of approximately 350 m in the center of the valley. As discussed above, the two closely spaced faults along the western and eastern margins of the valley may represent fault zones of many closely spaced, small-displacement faults. Along profile EE', there are no apparent reverse drag features. Real dips of the interpreted faults along EE' range between 14° and 33°.

Profile FF' (Figure 7) is 10 km across and begins along the western edge of Cedar Valley and ties into bedrock in the Mosida Hills to the east. A vertical displacement of approximately 250 m occurs along profile FF'. In contrast to profile EE' (Figure 6), the thickness of the tuff in this model is not uniform, but reaches a thickness of about 60 m near the middle of the valley and thins to 30 m and less toward the edges. This may be a depositional feature, but could also be due to erosion of the tuff along the margins of the valley before burial. The interpreted faults along FF' have real dips ranging from 18° to 36°.

Profile GG' (Figure 8) is 10 km long and begins in the Boulter Mountains to the west, extends eastward across Cedar Valley, and ends in the East Tintic Mountains. This profile is across the southern end of the valley and shows similar reverse drag faulting as profile DD' (Figure 5) at the northern end of the valley. Both sides of the valley have relatively steep dipping walls, suggesting the presence of faults, and the tuff has a uniform thickness of approximately 20 m. There are outcrops of tuff along the western and eastern margins of the valley in this area. From the model, it is concluded that these outcrops represent portions of the tuff sheet that were not downfaulted. This suggests that the north-striking normal faulting occurred after tuff deposition. Interpreted normal faults along the margins of the valley account for most of the approximately 200 m of vertical displacement. Real dips for the three interpreted faults along GG' range between 20° and 26°.

A fifth model was constructed across Goshen Valley along profile BB' (Figure 9). Because of existing power lines in this area, the collected magnetic data were rather sparse, so only the residual gravity data were used to construct this model. A classic stair-step fault model best fits the data. In addition, a graben structure along the western edge of Goshen Valley is also apparent. The stair-step faults account for approximately

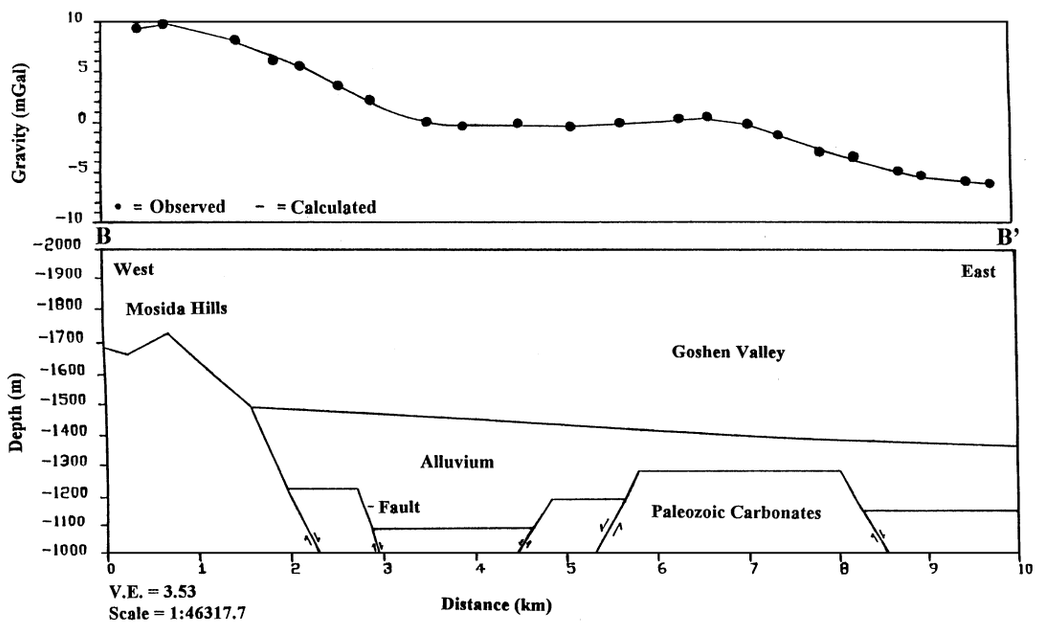

FIG. 9. Residual gravity along profile BB' (for location, see Figure 2). The modeled gravity are generated from a geological model showing a classic stair-step fault system. Power lines in this area allowed only sparse collection of magnetic data. The vertical exaggeration is 3.53, but none of the five interpreted faults have real dips less than 20°. Real dips ranged between 30° and 47°.

350 m of vertical offset, the graben adds an additional 50 m of vertical displacement. Real dips along BB' range from 30° to 47°, suggesting that folding and downwarping didn't play as much of a role in the formation of Goshen Valley as they did in the formation of Cedar Valley.

INTEGRATED INTERPRETATION OF CONCEALED FAULTS AND IGNEOUS BODIES

Using the subsurface models (Figures 5–9) as prototypes and the contoured data (Figures 3, 4), several range-bounding, normal faults have been interpreted (Figure 10). Due to the presence of some low-angle faults (real dips less than 20°), uncertainties in the fault locations extended to the surface may be up to 0.3–0.4 km from the interpreted plan view locations. The models indicate that there are faults along the western and eastern edges of Cedar Valley that stair-step away from the mountains toward the valley center. Furthermore, concealed normal faults associated with the Cedar Valley graben are interpreted beneath the valley floor. At the southwestern end of the valley, more data are needed to determine whether the westernmost fault bends eastward around the outcrop of Pennsylvanian-age carbonate rocks or cuts behind it making the outcrop a downdropped ridge. Based upon contours extending outside of the study area, it is assumed that it cuts behind the outcrop and continues southward into the East Tintic Mountains.

Geophysical evidence for a strike-slip fault in the vicinity of Chimney Rock Pass, as proposed by P. D. Proctor (unpublished data, 1985, 1990) from surface data, is not conclusive, but evidence for dip-slip movement along this trace exists in the gravity data. As mentioned earlier, two offset gravity highs in the Mosida Hills may represent strike-slip movement. However, it is uncertain whether this movement is toward the northeast, as Proctor suggests, or to the northwest, or possibly even to the east. It is also possible that the normal fault along the eastern edge of Cedar Valley intersects and joins with this fault forming a junction (Figure 10).

On the Goshen Valley/Utah Lake side of the range, there is an interpreted stair-step fault zone along the eastern edge of the East Tintic Mountains that strikes northward into the Mosida Hills, where it either terminates or there is an insufficient density contrast to produce an anomaly. This fault zone, along with a stair-step fault zone just west of the lava flow at L (Figure 4), forms a small graben. This graben extends southward and can be seen in the model along profile BB' (Figure 9). The existence of the stair-stepped faults forming the eastern boundary of this graben is indicated by modeling, a steep gravity gradient (Figure 3), and a 30-m cliff along the western edge of the lava flow located at L. Another normal fault appears to begin farther to the east near Utah Lake (Figures 9, 10). This concealed fault strikes northward through Goshen Valley and may connect with the fault that bends to the northeast along the eastern flank of the Lake Mountains (Figure 10).

There are three east-trending, steep gravity gradients (Figure 3): one on the north side of Chimney Rock Pass, one on the north end of the Mosida Hills, and one at the southern end of the Lake Mountains. It is possible that these also represent normal faults, but the one on the north side of Chimney Rock Pass is more subdued and could represent steep bedrock topography, a deeper depth to bedrock, or a smaller density contrast between rock types. Because the topography in the Mosida Hills area is fairly continuous across these faults, it is not likely that these east-striking faults are Basin and Range faults, but represent an earlier faulting episode.

From the magnetic data, surface-mapped mafic flows (J, K, and L; Figure 4) are each represented by a large localized anomaly. The magnetic data also indicate that there are three concealed igneous bodies, most likely mafic-to-intermediate composition lava flows, buried in Goshen Valley (X, Y, and Z; Figure 4). These bodies, varying in upper surface area from approximately 0.35 km^2 to 0.5 km^2 to 1.3 km^2, respectively, apparently originated from volcanic activity in the Mosida Hills. The southernmost body (Z; Figure 4) appears to be dipolar, containing some remanent magnetization. The concealed igneous body to the north (X; Figure 4) may also be dipolar and contain some remanent magnetization. In addition, the contoured magnetic data and the associated models (Figures 3–9) suggest that there is a large ash-flow tuff sheet, approximately 20 km^2 and 20–60 m thick, that is downfaulted and buried in Cedar Valley (Figures 5–8, 10).

PRACTICAL APPLICATIONS

Having obtained a better understanding of the location and nature of faulting and volcanics in the Mosida Hills area, there are many practical applications that result from the interpreted geophysical data.

Utah County officials are using the interpreted data to help develop future master plans for housing development in the Mosida Hills area, particularly in Goshen Valley. Minimization of earthquake-generated devastation requires candid communications between the scientific community, policy makers, and citizens; a thorough understanding of earthquake processes; identification of potentially active earthquake locations; and well-defined mitigation procedures. Locations of potential geological hazards taken from the geophysical maps in this study are helping create adequate setback zones from fault lines for the construction of buildings (N. Jones, personal communication, 1999).

Although the risk of volcanic-related threats in the Mosida Hills is low, ignoring the threats could increase the level of damage during an emergency and expand economic devastation to nearby communities. Understanding volcanic processes, locations of lava flows, and identification of potentially active eruptive vents associated with mapped lava flows are helping formulate mitigation procedures for the Mosida Hills area (N. Jones, personal communication, 1998; B. Rose, personal communication, 1999).

In the southern portion of the study area, both west and east of the East Tintic Mountains (Figure 2), potential mineral deposits associated with interpreted fault locations and buried igneous bodies are being assessed (P. D. Proctor, unpublished data, 1998). Similar assessments are being made in the northern part of the study area, west of the Lake Mountains (Figure 2). Silver, zinc, and lead are associated with some of the deposits (P. D. Proctor, unpublished data, 1998; G. E. Christenson, personal communication, 1998).

Gravity highs associated with faulted bedrock in Cedar Valley are being investigated as potential hydrocarbon traps (T. C. Chidsey, personal communication, 1999). Minimally, this geophysical survey creates a regional basis for more detailed petroleum studies in eastern and western portions of Cedar Valley. A well east of the Mosida Hills area produced some hydrocarbon shows (Benson and Hash, 1998).

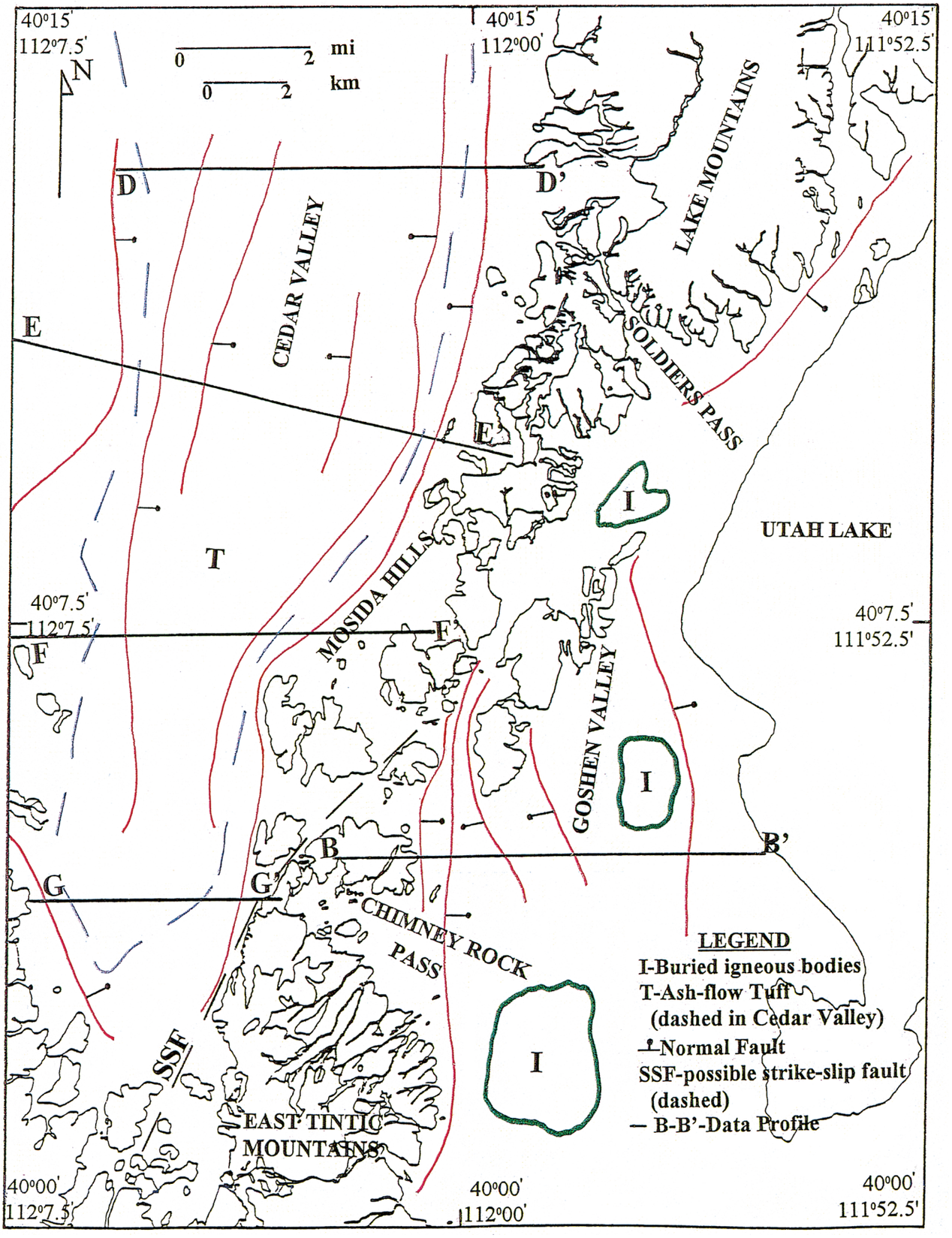

FIG. 10. Map of concealed faulting, buried igneous bodies (I, outlined in green), and buried ash-flow tuff (T, dashed blue outline in Cedar Valley) interpreted from the gravity and magnetic data. Eleven normal faults (or fault segments) are mapped (red lines), as well as a possible strike slip fault (SSF, dashed). Due to some low-angle faults and uncertainties in the models, extended fault locations may have a surface location uncertainty up to 0.3–0.4 km on this plan view map.

CONCLUSIONS

Gravity and magnetic data were collected, processed, and interpreted to help identify and better understand concealed geological structures in the Mosida Hills area. The integration of gravity and magnetic data led to the interpretation of eleven normal faults (or fault segments) in the Mosida Hills area. Ambiguities in the geological models were reduced by (1) incorporating data from previous geophysical surveys, surface mapping, and aeromagnetic data, (2) integrating the gravity and magnetic data from our survey, and (3) correlating the modeled cross sections. Eight of the interpreted faults (or fault segments) are concealed and were previously unmapped and/or unknown.

Modeled normal faults beneath Goshen Valley show vertical displacements of 350 m to more than 400 m. Furthermore, four concealed normal faults associated with the Cedar Valley graben show vertical displacements on the faults that range from 200 to 350 m, increasing toward the north. Since approximately one-third of the interpreted faults in Cedar Valley have real dips less than 20°, folding and downwarping, in addition to faulting, likely played an important role in the formation of Cedar Valley. Although evidence for a strike-slip fault in the vicinity of Chimney Rock Pass was not conclusive, a fault at that location is probable, being associated with two offset gravity highs. The gravity data indicate that is highly probable that this fault has a component of dip-slip movement.

From the magnetic data, three previously unknown igneous bodies were interpreted beneath Goshen Valley. All three bodies may be dipolar and contain some residual magnetization. In addition, the magnetic data suggest the existence of a large ash-flow tuff that is downfaulted and buried in Cedar Valley. Thicknesses of this modeled tuff range between 20 and 60 m, while the upper surface area is approximately 20 km^2.

The interpreted location and nature of concealed faults and volcanic flows in the Mosida Hills area are being used by policy makers to help develop mitigation procedures to protect life and property, particularly in Goshen Valley. Furthermore, potential hydrocarbon traps and mineral deposits associated with some of the interpreted geologic structures in eastern and western portions of Cedar Valley are being evaluated and assessed for possible future development.

ACKNOWLEDGMENTS

Our appreciation is extended to R.O. Hansen, R. Pawlowski, and other reviewers for their insightful comments and suggestions on this manuscript.

REFERENCES

Benson, A. K., and Hash, S. T., 1998, Integrated three-dimensional interpretation of major concealed faults beneath Mapleton, Utah County, Utah using gravity data, supported with magnetic data: Eng. Geol., **51**, 109–130.

Benson, A. K., and Mustoe, N. B., 1991, Delineating concealed faults and shallow subsurface geology along the Wasatch Front, Utah, USA, by integrating geophysical and trench data: Quart. J. Eng. Geol., **24**, 375–387.

——— 1995, Analyzing shallow faulting at a site in the Wasatch fault zone, Utah, USA, by integrating seismic, gravity, magnetic, and trench data: Eng. Geol., **40**, 139–156.

Bullock, K. C., 1951, Geology of Lake Mountain, Utah County, Utah: Geol. Min. Surv. Bull., **41**.

Burger, H. R., 1992, Exploration geophysics of the shallow subsurface: Prentice Hall, Inc.

Cook, K. L., and Berg, J. W., 1961, Regional gravity survey along the central and southern Wasatch Front Utah: U.S. Geol. Surv. Prof. Paper **316-E**.

Cook, K. L., Edgerton, D. A., Serpa, L. F., and DePangher, M., 1997, Complete Bouguer gravity anomaly map and geological interpretation of the southern Wasatch Front, Utah: Utah Geol. Surv. Report **97-1**.

Davis, D. A., 1983, Gravity survey of Utah and Goshen Valley and adjacent areas, Utah: Master's thesis, Univ. of Utah.

Dobrin, M. B., and Savit, C. H., 1988, Introduction to geophysical prospecting: McGraw-Hill.

Gori, P. L., 1993, Interactive workshops: Essential elements of the earthquake hazards research and reduction program in the Wasatch Front, Utah, *in* Gori, P. L., Ed., Applications of research from the U.S. Geological Survey Program, assessment of regional earthquake hazards and risk along the Wasatch Front, Utah: U.S. Geol. Surv. Prof. Paper **1519**, 1–7.

Hamblin, W. K., 1965, Origin of "reverse drag" on the downthrown side of normal faults: Geol. Soc. Am. Bull., **76**, 1145–1164.

Hintze, L. F., 1988, Geologic history of Utah: Brigham Young Univ. Geology Studies Special Publication 7.

Hoffman, F. H., 1951, Geology of the Mosida Hills area, Utah: Master's thesis, Brigham Young Univ.

Morris, H. T., and Lovering, T. S., 1961, Stratigraphy of the East Tintic Mountains, Utah: U.S. Geol. Surv. Prof. Paper **361**.

Parasnis, D. S., 1962, Principles of applied geophysics: Methuen.

Rigby, J. K., 1949, Stratigraphy and structure of the Paleozoic rocks in the Selma Hills, Utah County, Utah: Master's thesis, Brigham Young Univ.

——— 1952, Geology of the Selma Hills, Utah County, Utah: Utah Geol. Min. Surv. Bull., **45**.

Robinoson, R. M., 1993a, Surface-fault rupture: A guide for land-use planning, Utah and Juab Counties, Utah, *in* Gori, P. L., Ed., Applications of research from the U.S. Geological Survey Program, assessment of regional earthquake hazards and risk along the Wasatch Front, Utah: U.S. Geol. Surv. Prof. Paper **1519**, 121–128.

——— 1993b, Tectonic subsidence hazard: A guide for land-use planning, Utah and Juab Counties, Utah, *in* Gori, P. L., Ed., Applications of research from the U.S. Geological Survey Program, assessment of regional earthquake hazards and risk along the Wasatch Front, Utah: U.S. Geol. Surv. Prof. Paper **1519**, 158–162.

Stewart, J. H., 1983, Cenozoic structure and tectonics of the northern Basin and Range Province, California, Nevada, and Utah: Geothermal Resources Council Special Report **13**, 25–40.

Telford, W. M., Geldart, L. P., and Sheriff, R. A., 1990, Applied Geophysics, 2nd ed.: Cambridge Univ. Press.

White, P. H. N., 1949, Gravity data obtained in Great Britain by the Anglo-American Oil Co., Ltd.: Quart. J. the Geol. Soc. London, **104**, 339–364.

Williams, F. E., 1951, Geology of the north Selma Hills area, Utah County, Utah: Master's thesis, Brigham Young Univ.

Zeng, H., 1989, Estimation of the degree of polynomial fitted to gravity anomalies and its application: Geophys. Prosp., **37**, 959–973.

Zoback, M. L., 1983, Structure and Cenozoic tectonism along the Wasatch fault zone, Utah: Geol. Soc. of Am., Memoir **152**, 3–27.